European Research Council
Established by the European Commission

HELMHOLTZ CENTRE POTSDAM
GFZ GERMAN RESEARCH CENTRE FOR GEOSCIENCES

Improving the accuracy of geodesy and astrometry by VLBI Global Observing System

Ming Hui Xu

GFZ, Germany

13 November 2024, Radio 2024
Erlangen, Germany

Geodetic and astrometric VLBI

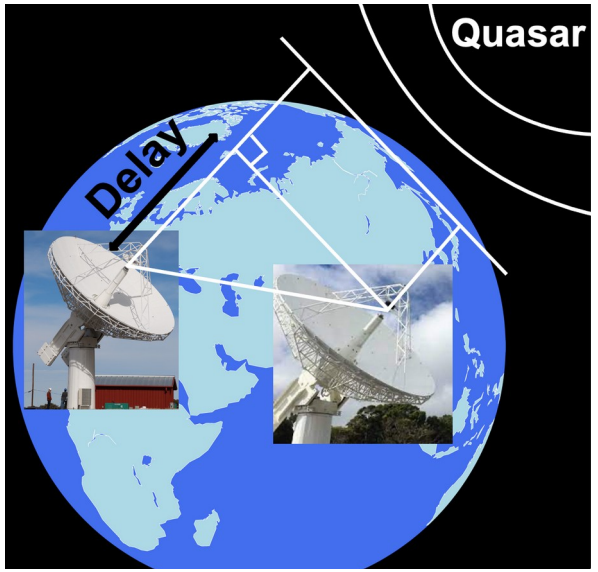

Global terrestrial reference frame

VGOS station network

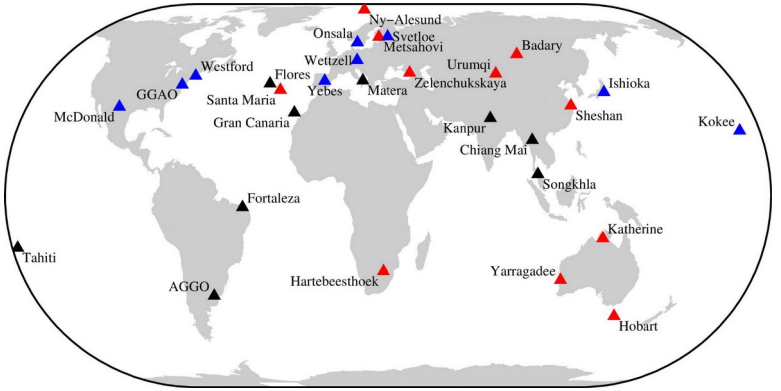

Status: Observing; Testing; Constructing

Regular observations with worldwide distributed antennas since 1979

- A network of typically 7 to 15 antennas
- Observing 24 hours per day and 4 days per week
- Tens to hundreds of AGNs in 24 hours

New generation geodetic VLBI since 2019

- Called VLBI Global Observing System (VGOS)
- Simultaneously observing at four bands 3 – 11 GHz

Quasars are lighthouses of VLBI

Earth and quasars

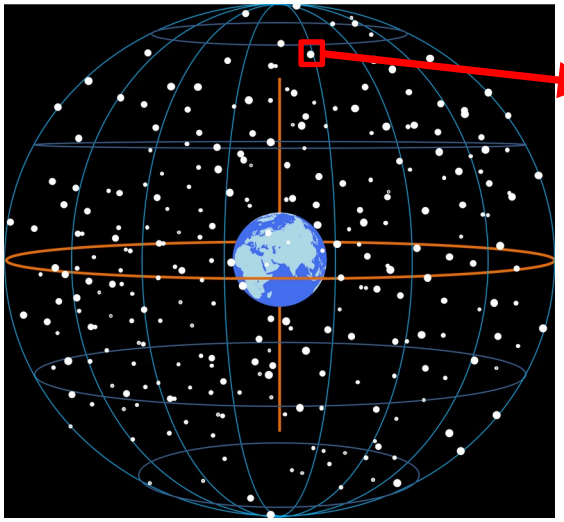

Assumption:
They are point like

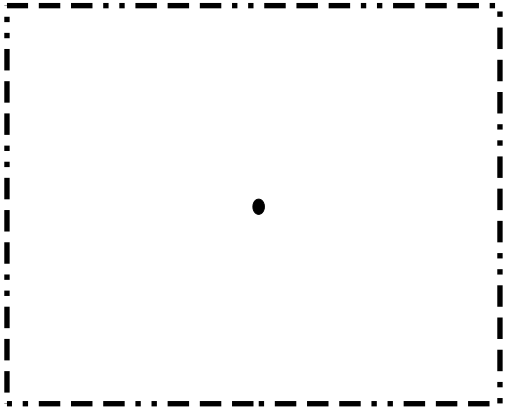

A real quasar: time- and frequency-dependent structure

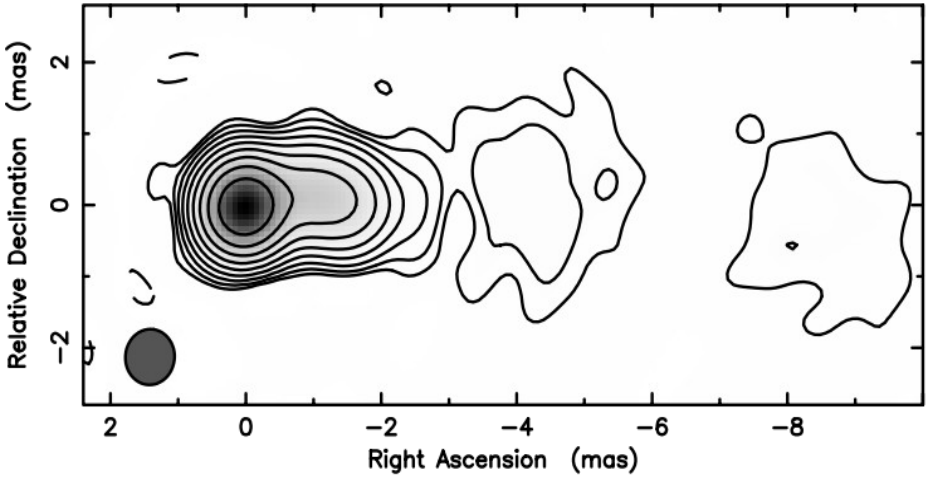

(***Xu*** et al., JGR, 2021; A&A, 2022)

One major systematic error is the un-modeled effects due to source structure.

Effects of source structure in VGOS

- Variations in absolute astrometric positions of AGNs
- Extra structure delays in the group delay observables
- Enlarging the measurement noise due to resolved structure
- Sub-ambiguities
- ……

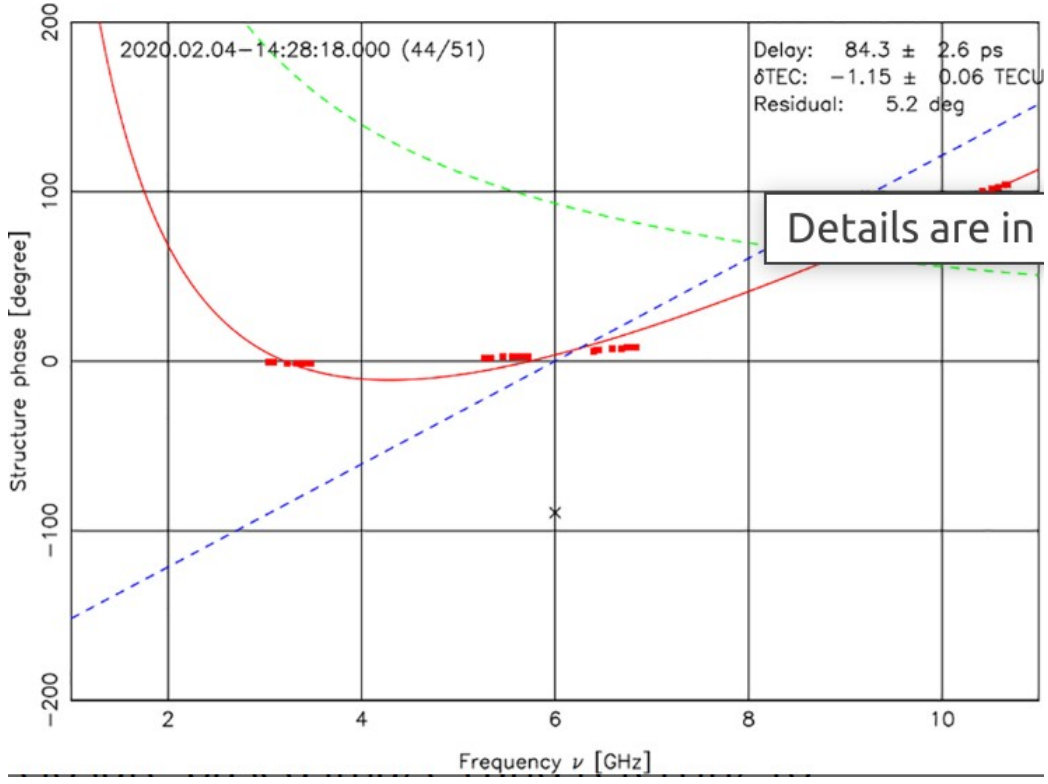

(Xu et al., 2021)

Effects of source structure in VGOS

- **Variations in absolute astrometric positions of AGNs**
- Extra structure delays in the group delay observables
- Enlarging the measurement noise due to resolved structure
- Sub-ambiguities
- ……

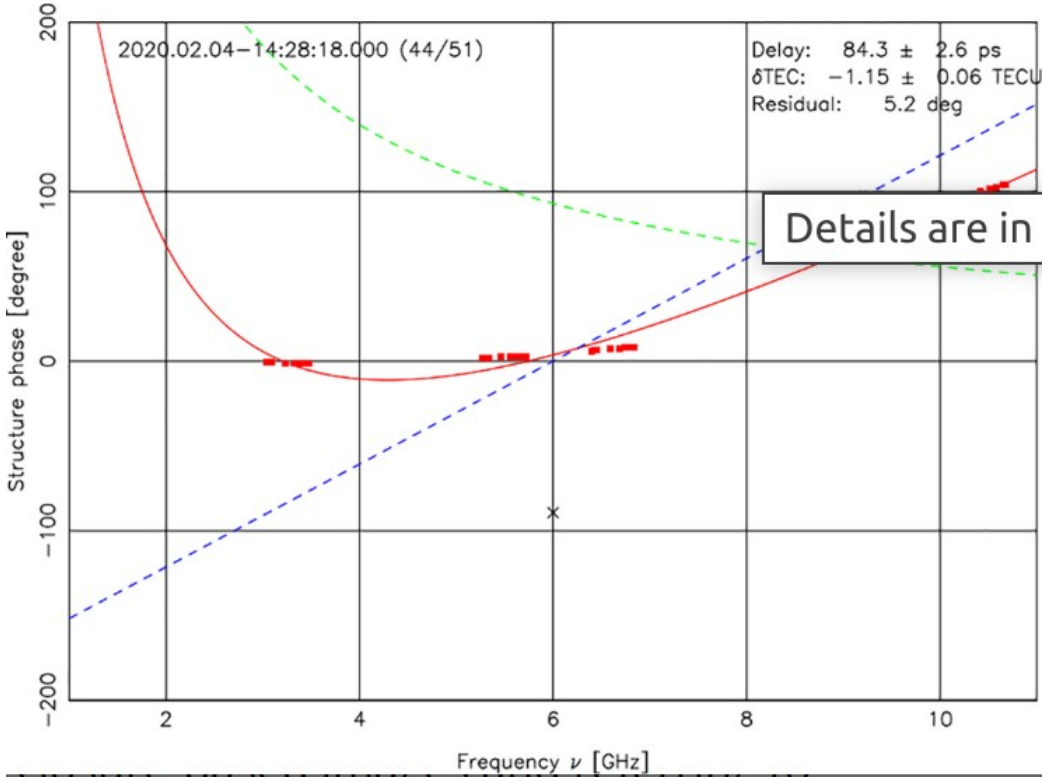

(Xu et al., 2021)

Data and data analysis

- **Data**
  - 177 VGOS sessions
  - 377 AGNs
- **Imaging**
  - Closure phases
  - Closure amplitudes
- **Geodetic analysis**
  - Independent solutions
  - Global solutions

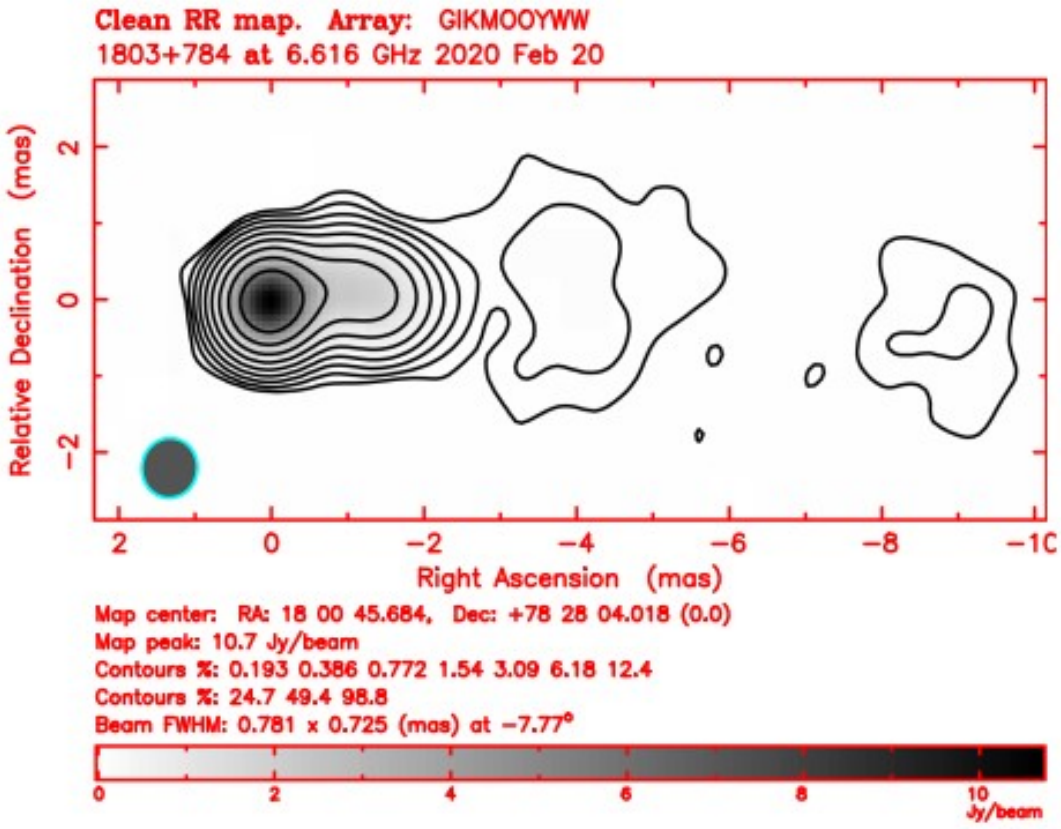

Source image of 1803+784 at 6.6 GHz from session VO0051 (Xu et al., 2021)

Stable at the level of ten micro-arcseconds

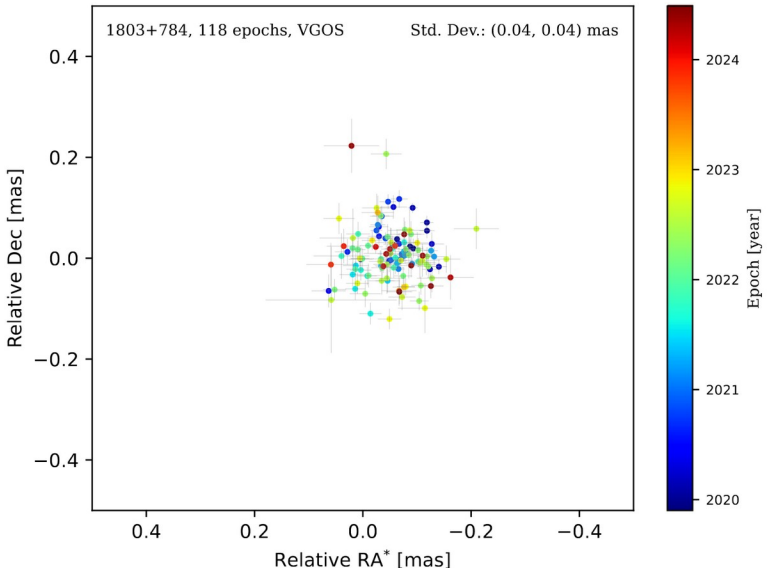

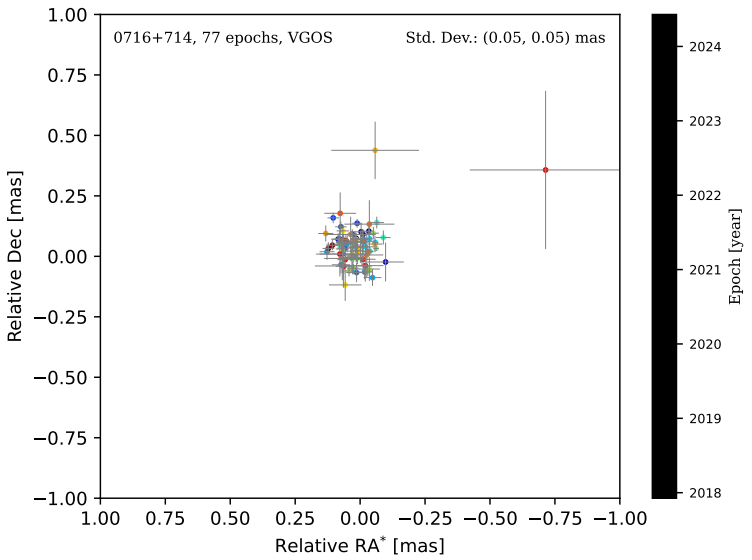

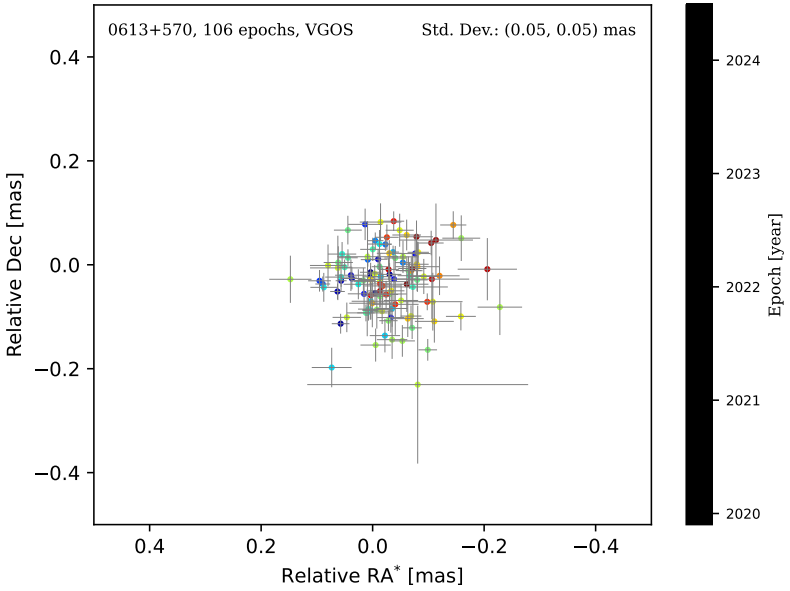

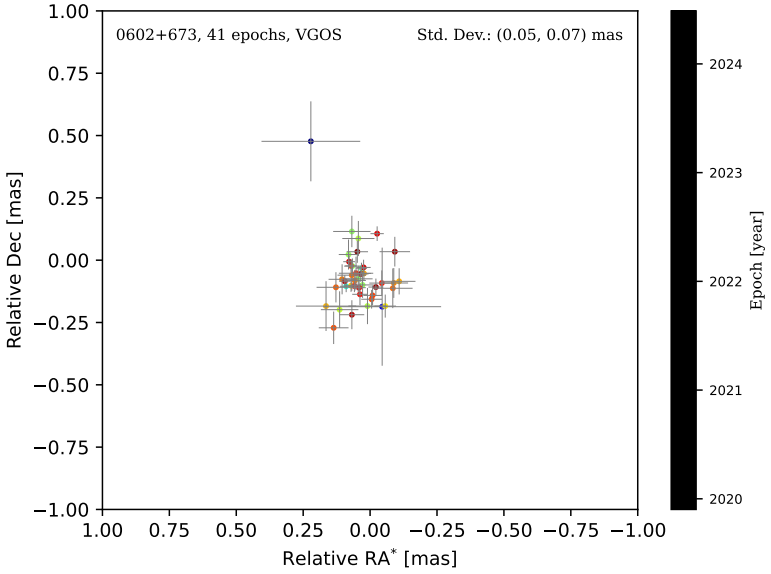

(Xu, submitted)

Stable: 1803+784

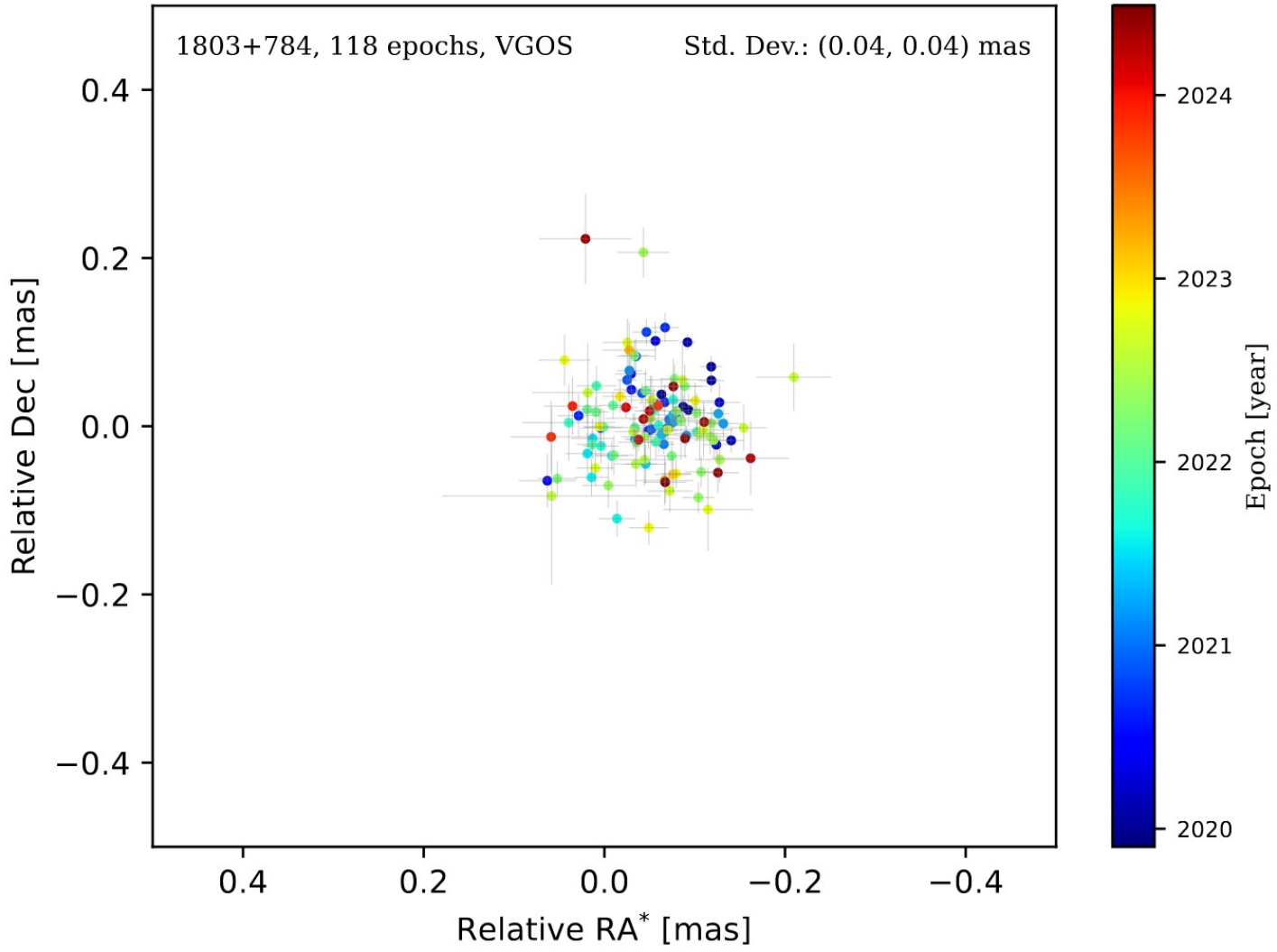

One direction moving

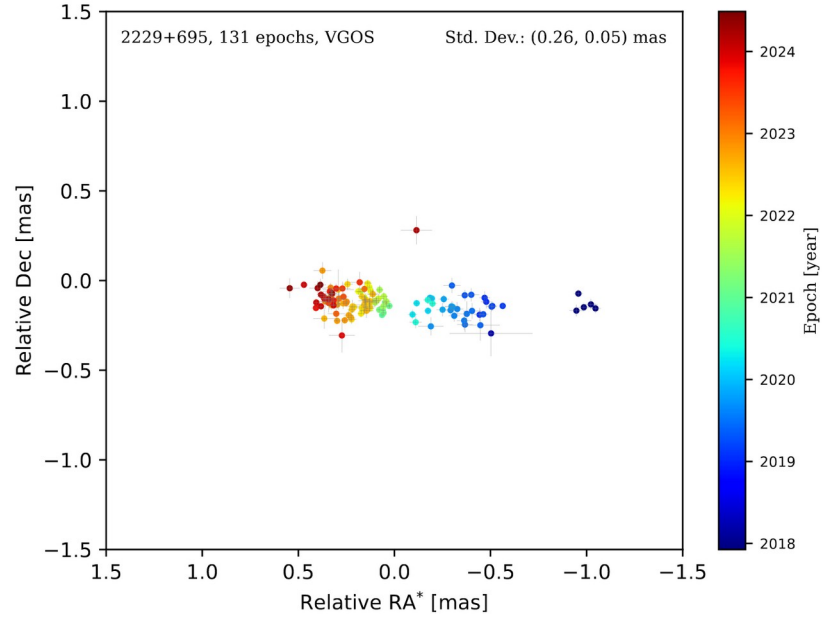

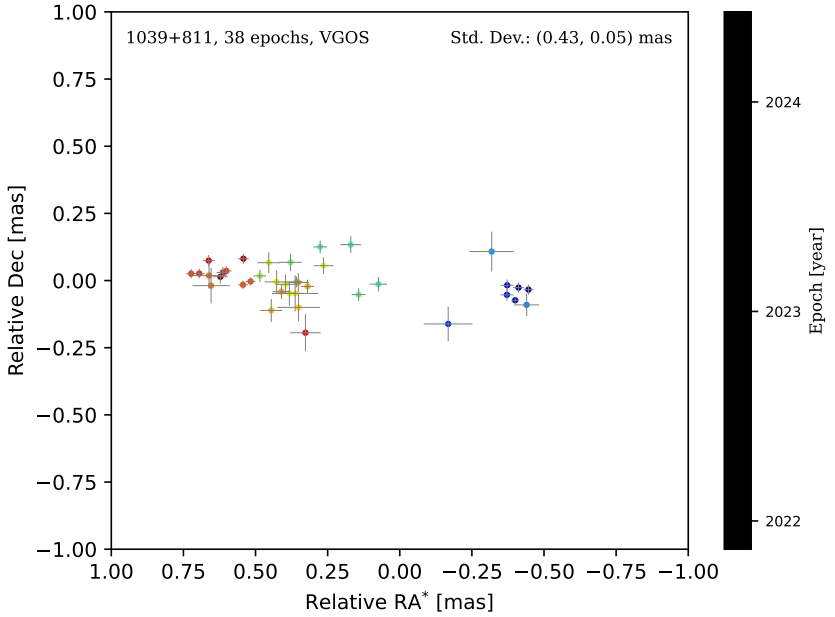

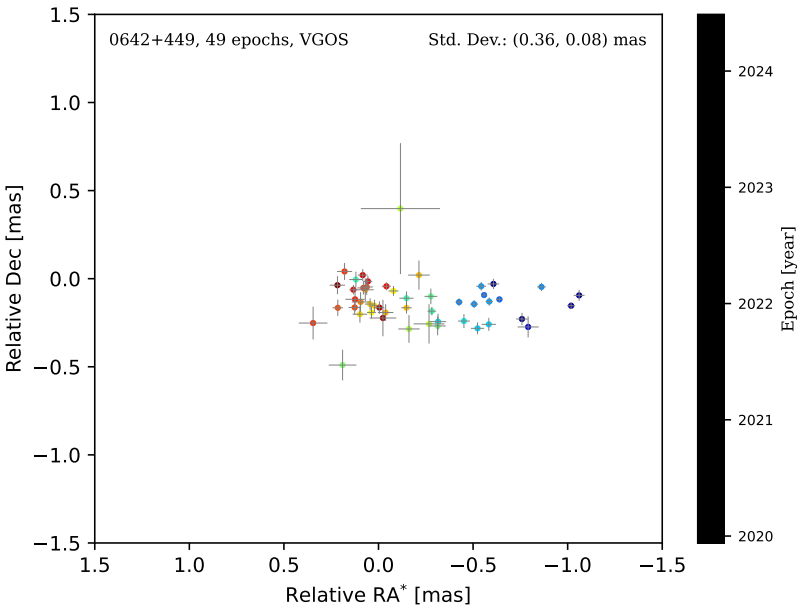

(Xu, submitted)

One direction moving: 2229+695

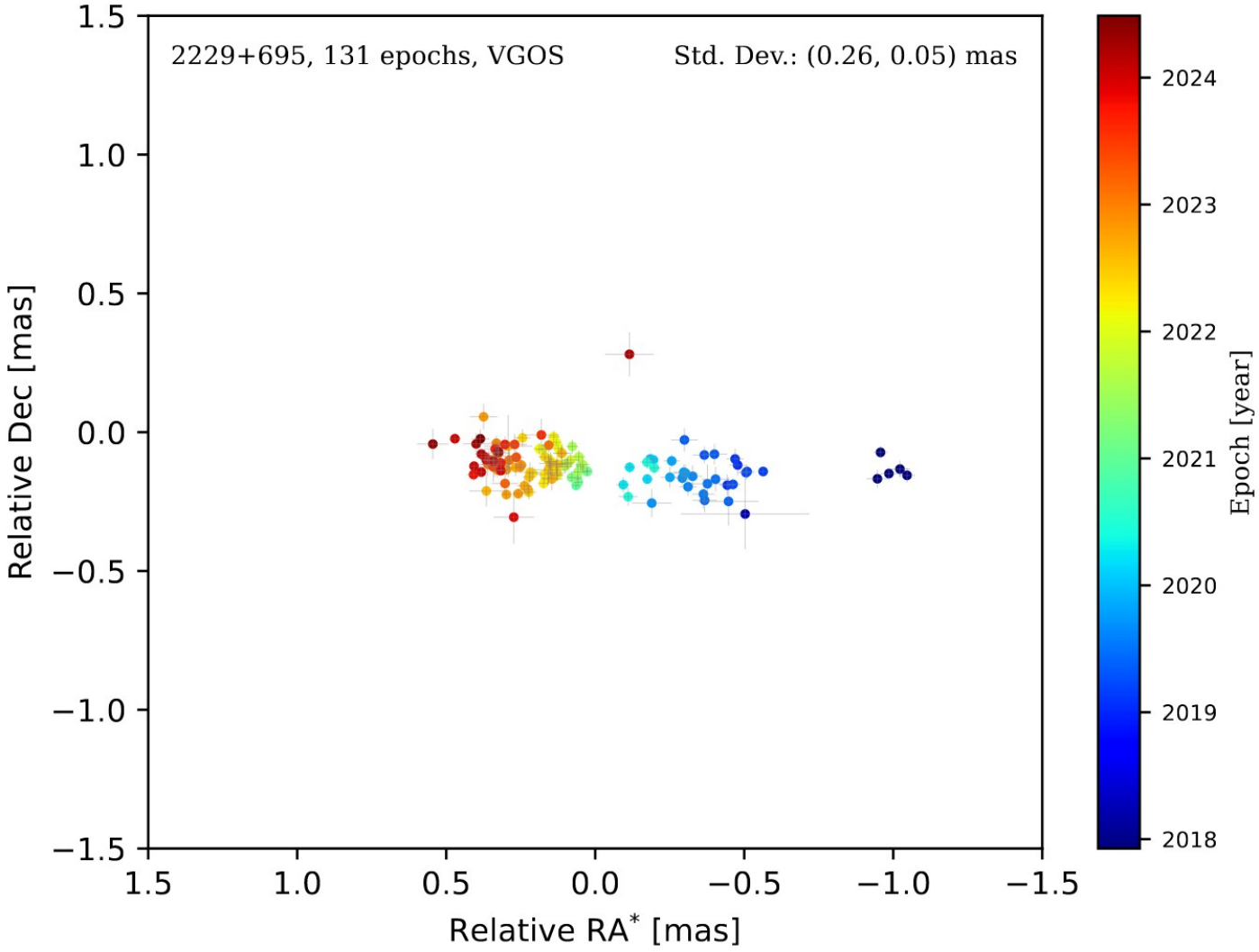

One direction moving: 2229+695

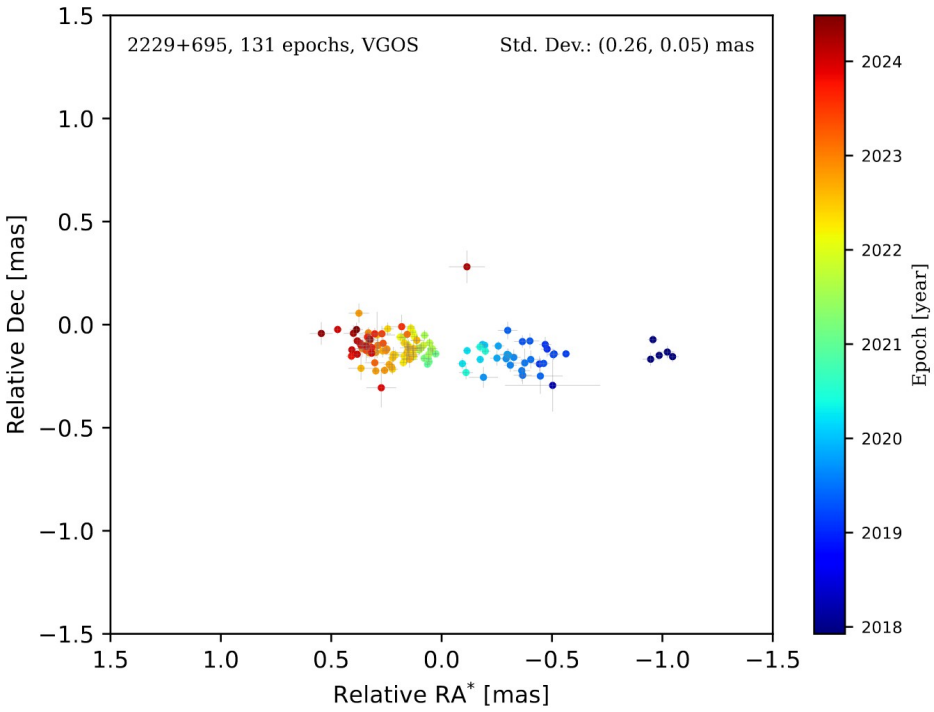

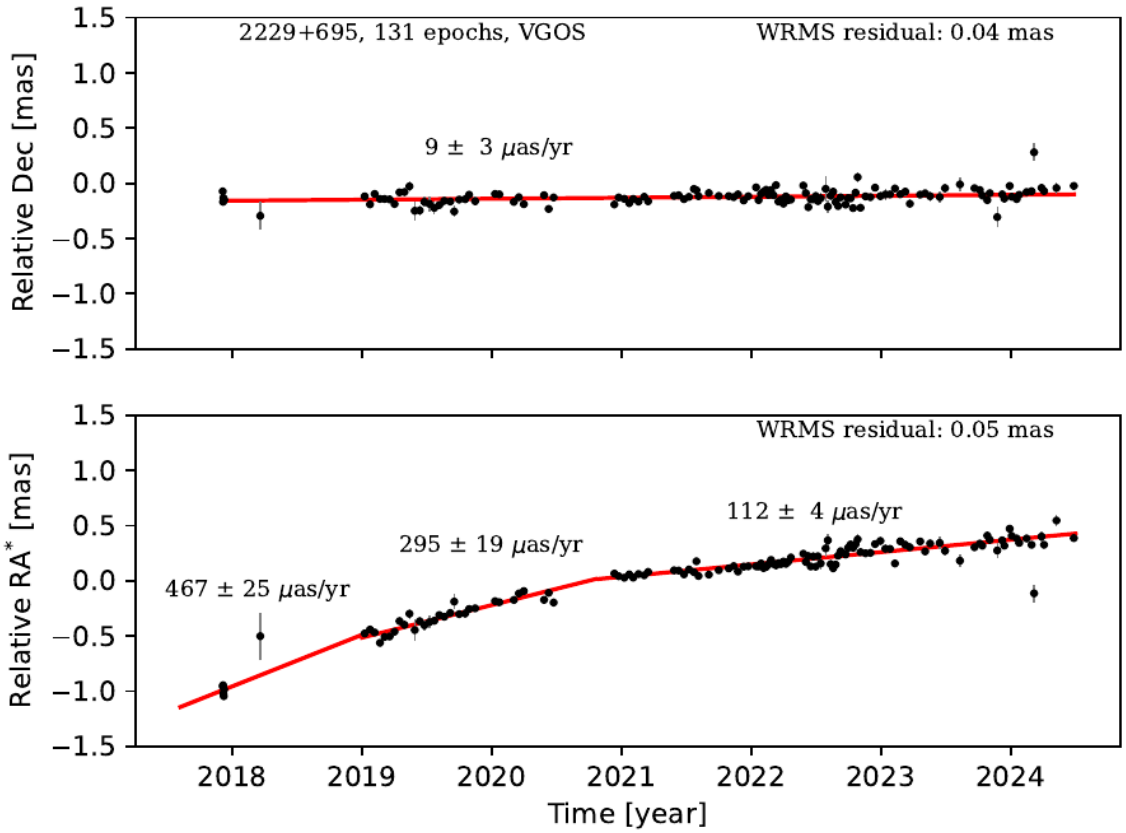

One direction moving: 2229+695

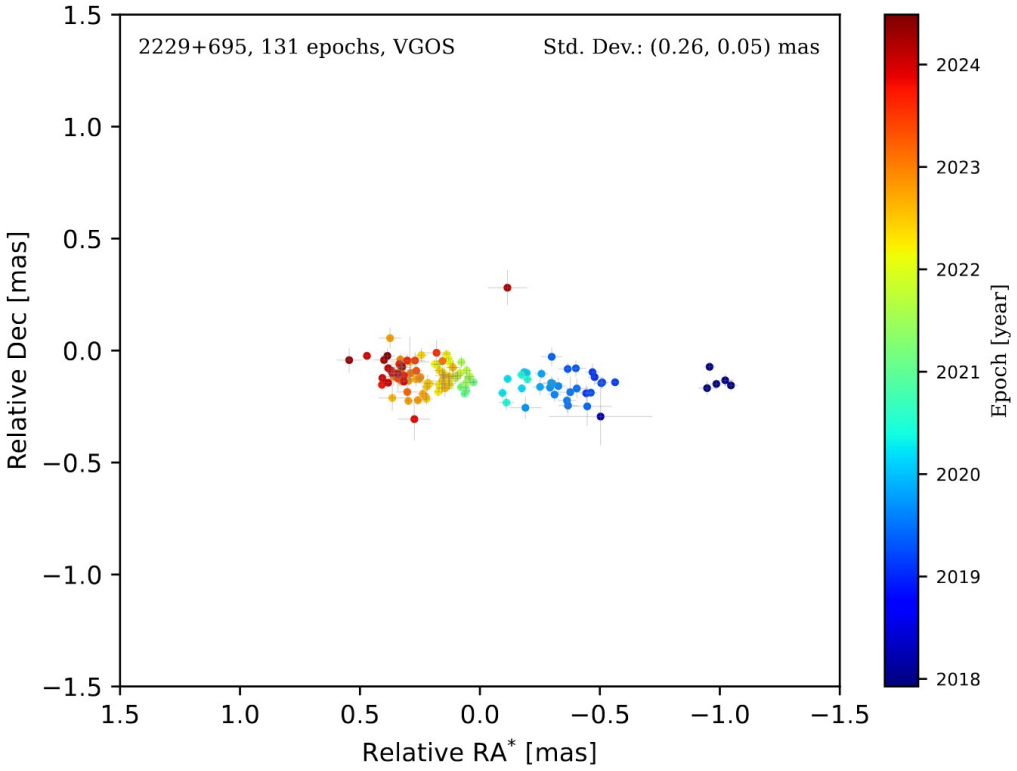

2022 JAN 27

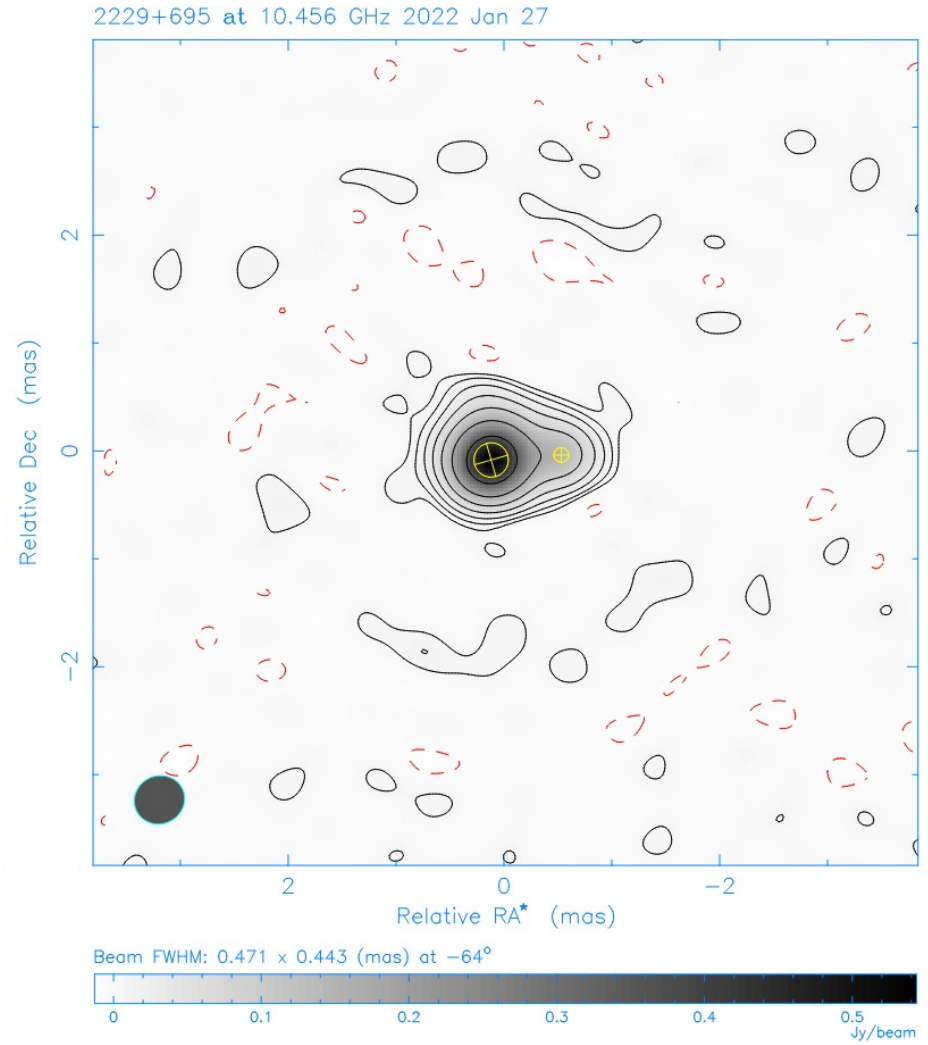

One direction moving: 2229+695

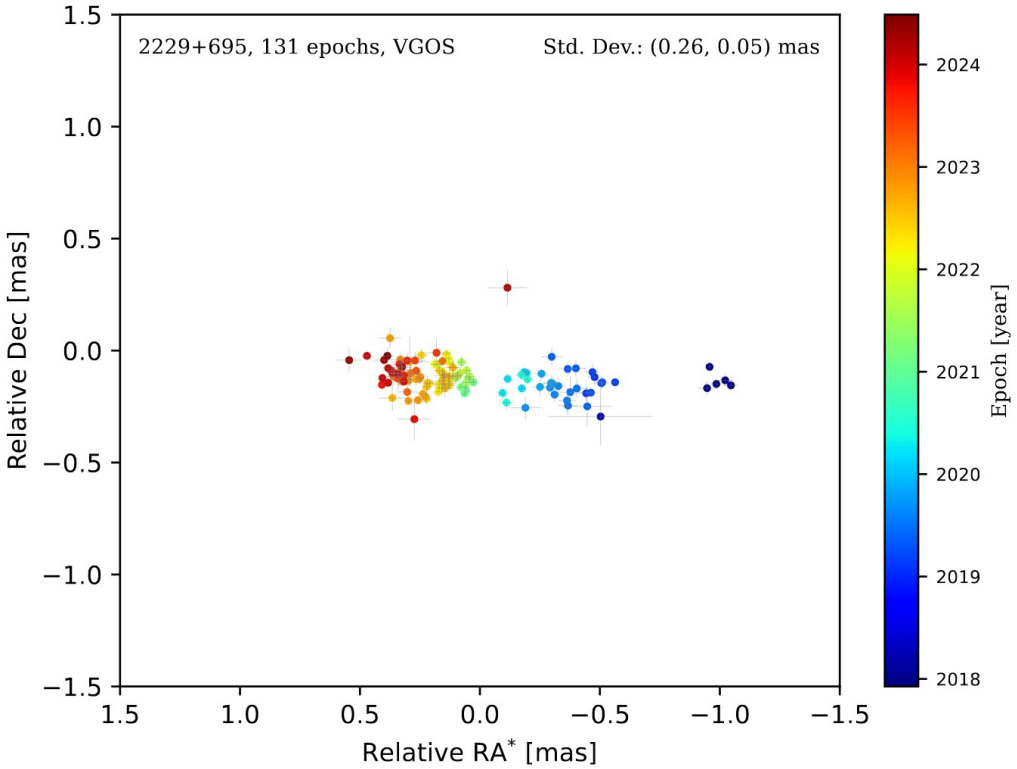

2022 JAN 27

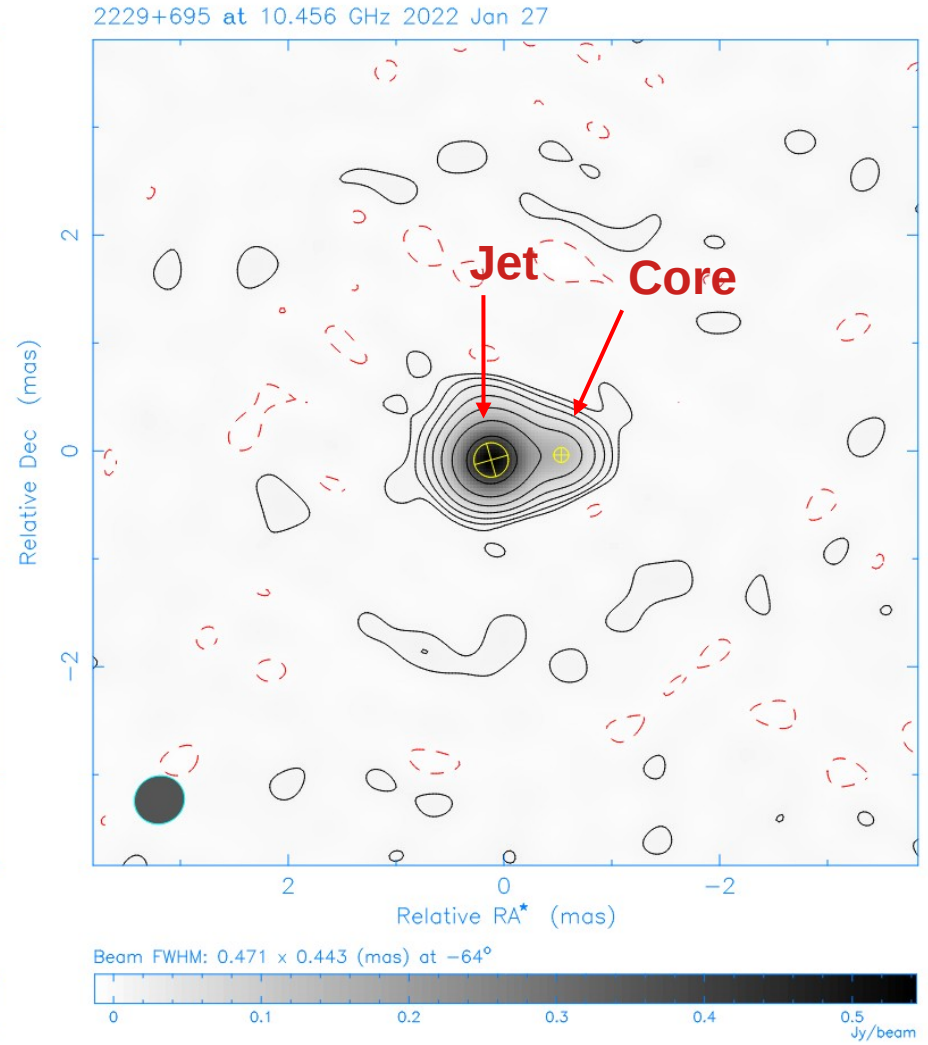

Two direction moving

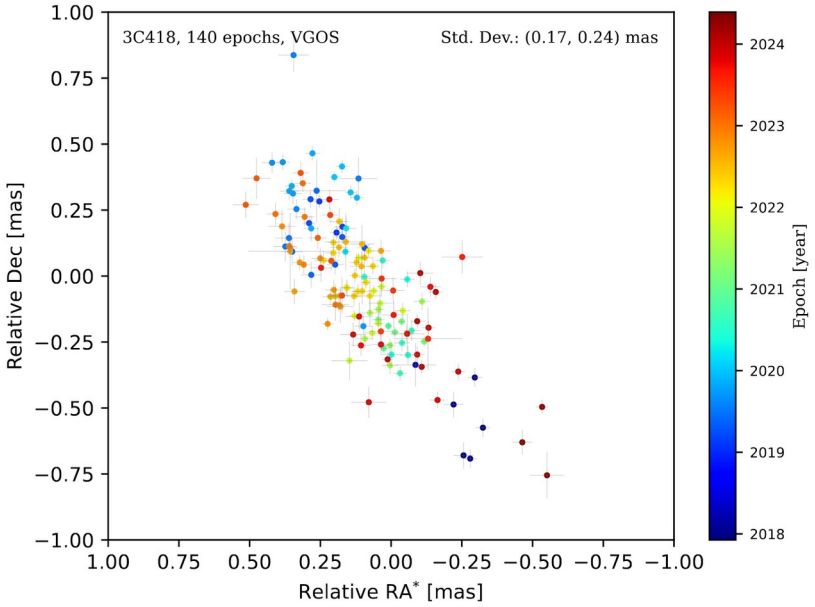

Two direction moving: 3C418

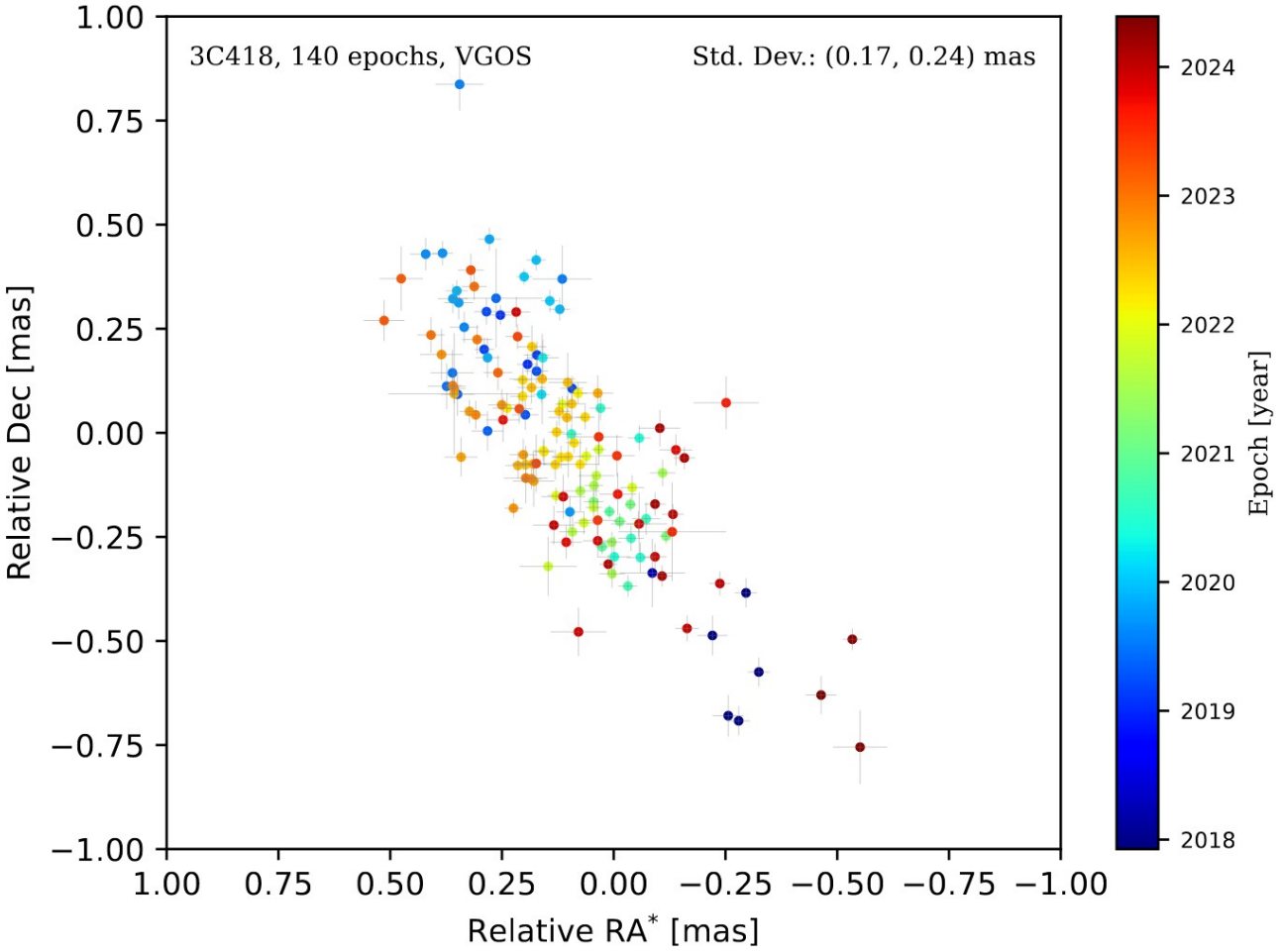

- Source position changes in its jet direction
  - Move towards east-north and west-south back twice from 2018 to 2024
  - Angular difference 1.1 mas
  - Typical behavior due to within beamsize structure

3C418: images

5.5 GHz

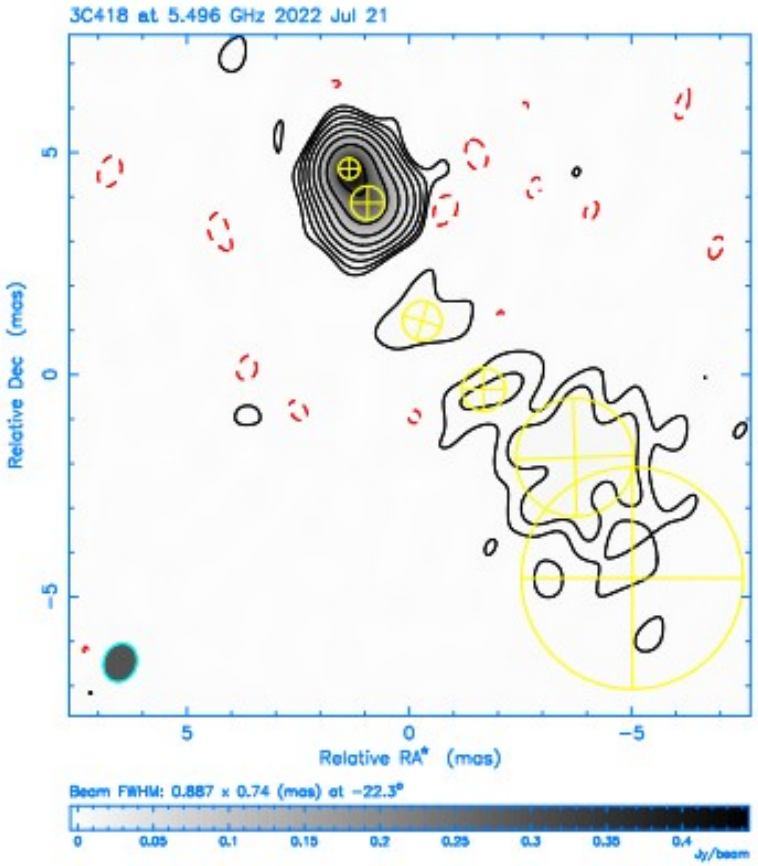

10.2 GHz

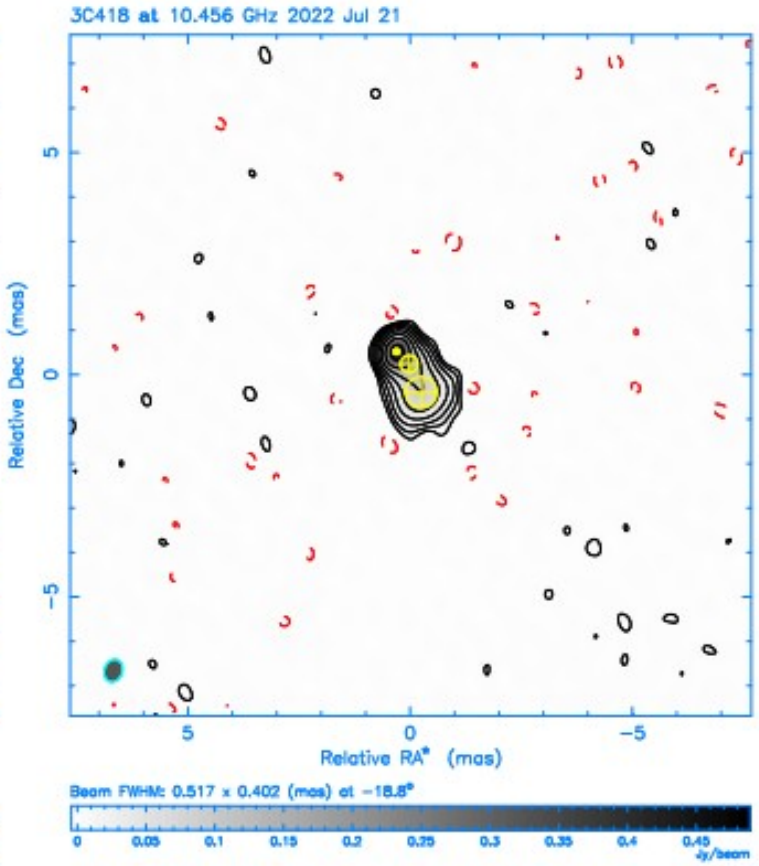

- VGOS beam size
  - 1.8 mas @ 3 GHz
  - 1.0 mas @ 5 GHz
  - 0.9 mas @ 6 GHz
  - 0.5 mas @ 10.5 GHz

- Extended structure at higher frequencies is un-resolved shifting the astrometric positions
- Image alignment over frequency

Source position variations across frequency

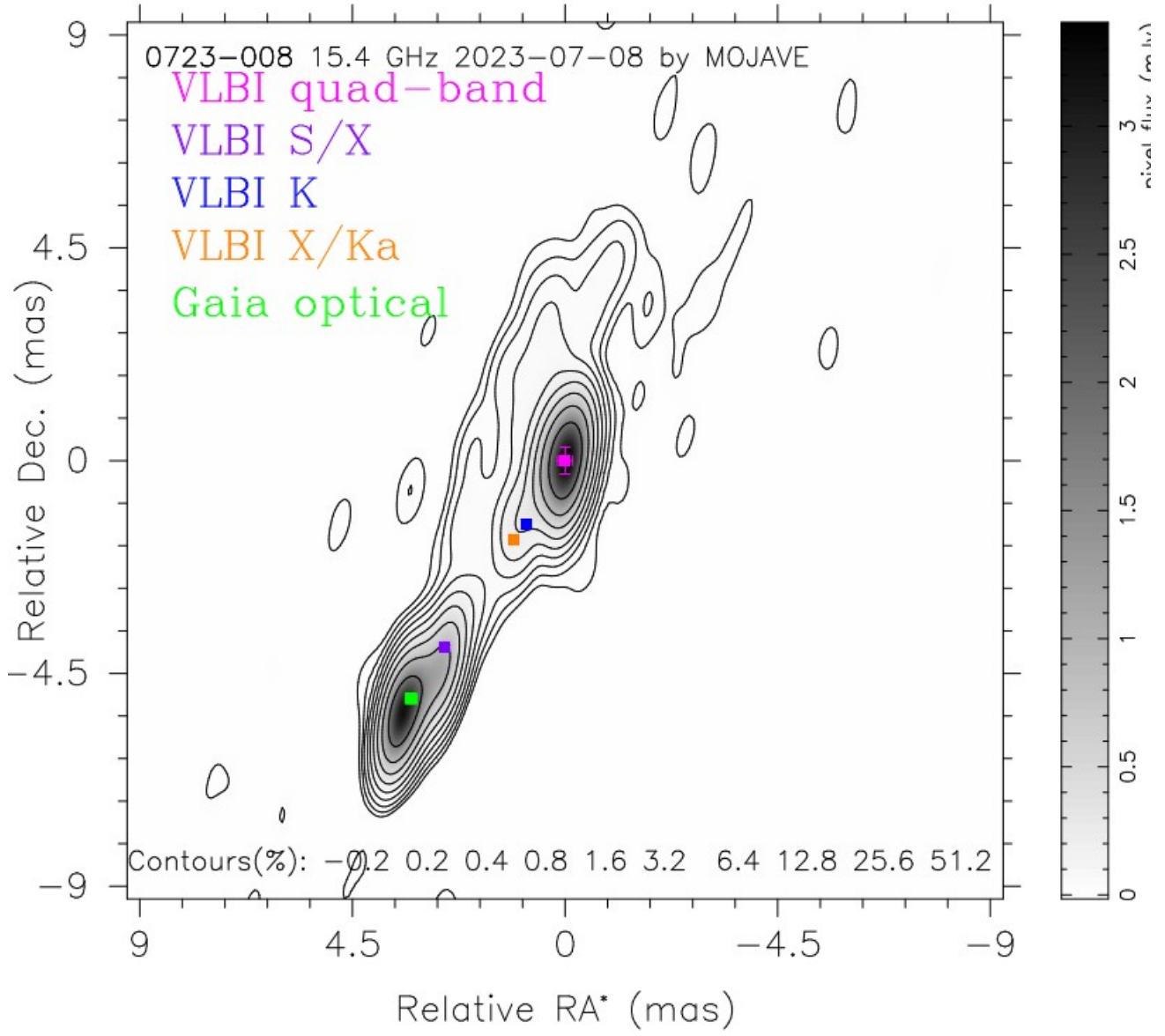

How to build a consistent CRF across frequency in the future?

MOJAVE as testbed

- Processing MOJAVE observations in geodetic mode
- Collaboration with MOJAVE team
  - models of source structure
  - Images aligned over time

Results from 147 MOJAVE sessions since 2012

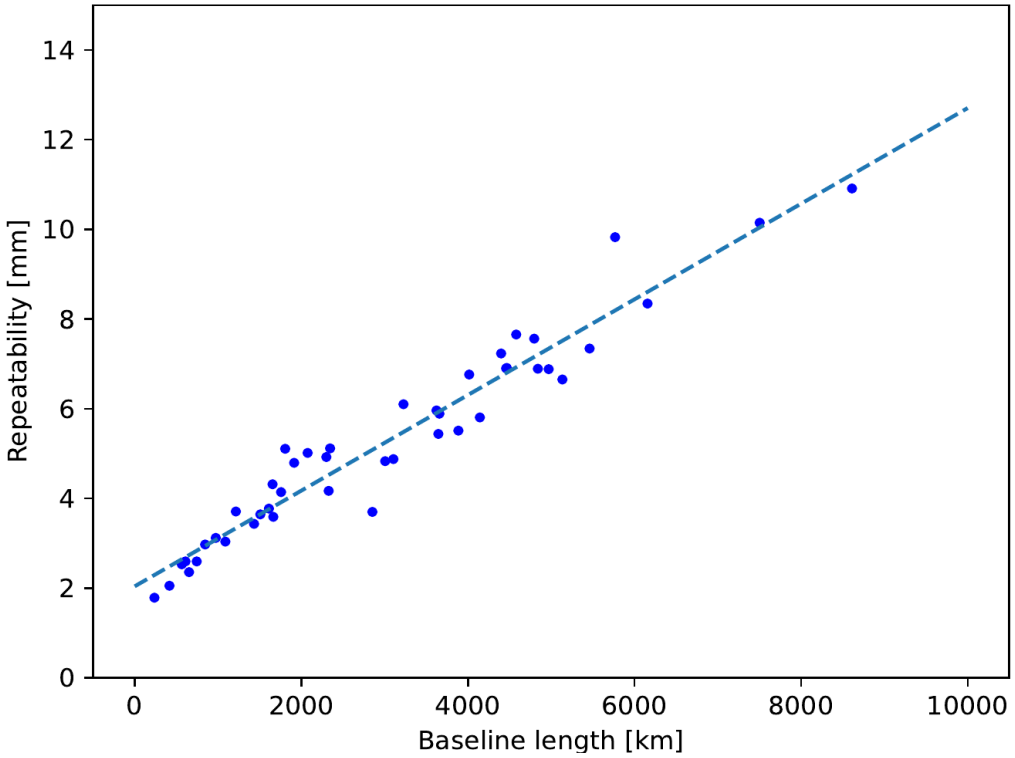

Baseline length repeatability degrades significantly with the length

(Lister etal., 2018)

Conclusion

1) Precision/white noise in VGOS source position < 40 *u*as

2) Contribution of source structure @ 0.1 – 0.2 mas

3) Astrogeodesy project aims to resolve this challenge for improving the accuracy of geodesy and astrometry

4) It is relevant for astrometry in the future radio facilities, like ngVLA

VGOS CRF

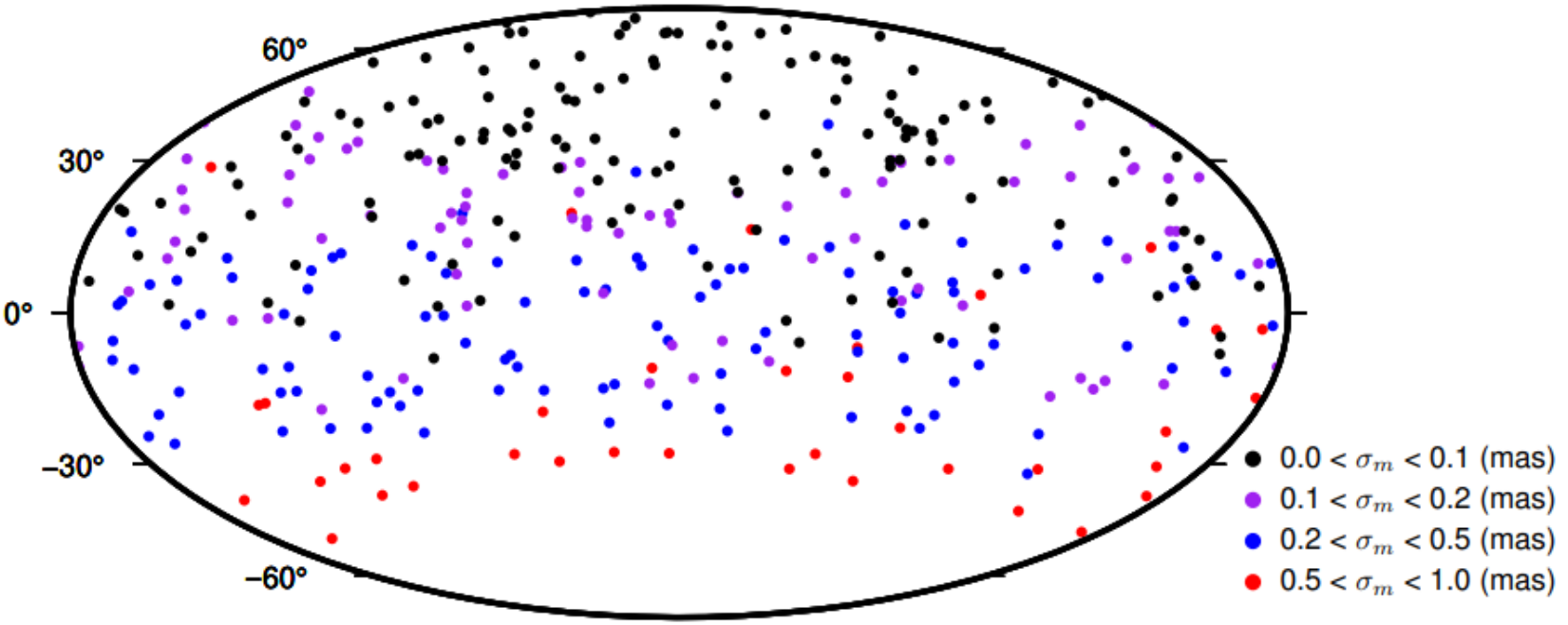

Source identification		Cat.	Right ascension	Declination	Coordinate uncertainty		Correl.	Epoch of sessions			Observations		
ICRF designation	IERS name		(h m s)	(° ′ ″)	(s)	(″)		Mean	First	Last	N_{ses}	N_{del}	N_{rat}
(1)	(2)	(3)	(4)	(5)	(6)	(7)	(8)	(9)	(10)	(11)	(12)	(13)	(14)
VGOS J000613.8−062335	0003−066		00 06 13.89288695	−06 23 35.3356525	0.00000244	0.0000842	−0.6000	59628.5	58910.0	60347.0	4994	52	0
VGOS J001708.4+813508	0014+813		00 17 08.47496488	+81 35 08.1353147	0.00002159	0.0000520	0.0670	60305.5	60264.0	60347.0	366	2	0
VGOS J001937.8+202145	0017+200		00 19 37.85449104	+20 21 45.6444849	0.00000085	0.0000277	−0.3970	59649.5	58812.0	60487.0	12768	97	0
VGOS J001945.7+732730	0016+731		00 19 45.78630761	+73 27 30.0176140	0.00000146	0.0000060	−0.0130	59278.0	58090.0	60466.0	43421	82	0
VGOS J002232.4+060804	0019+058		00 22 32.44120513	+06 08 04.2689689	0.00000167	0.0000637	−0.5220	59649.5	58812.0	60487.0	4952	87	0
VGOS J002829.8+200026	0025+197	D	00 28 29.81847340	+20 00 26.7439553	0.00000226	0.0000755	−0.2880	59623.0	58857.0	60389.0	1658	30	0

NOTE—Column (1) is the ICRF name with replacement of the first four characters to VGOS. In column (3), character "D" stands for the datum sources and "S" for the sources with positions as local parameters. The positions of the sources with character "S" are the mean estimates of these local positions. Columns (12) and (13) are the number of sessions and used observations, respectively. Column (14) is the number of delay rate observations and is kept only for consistency

Effects of source structure

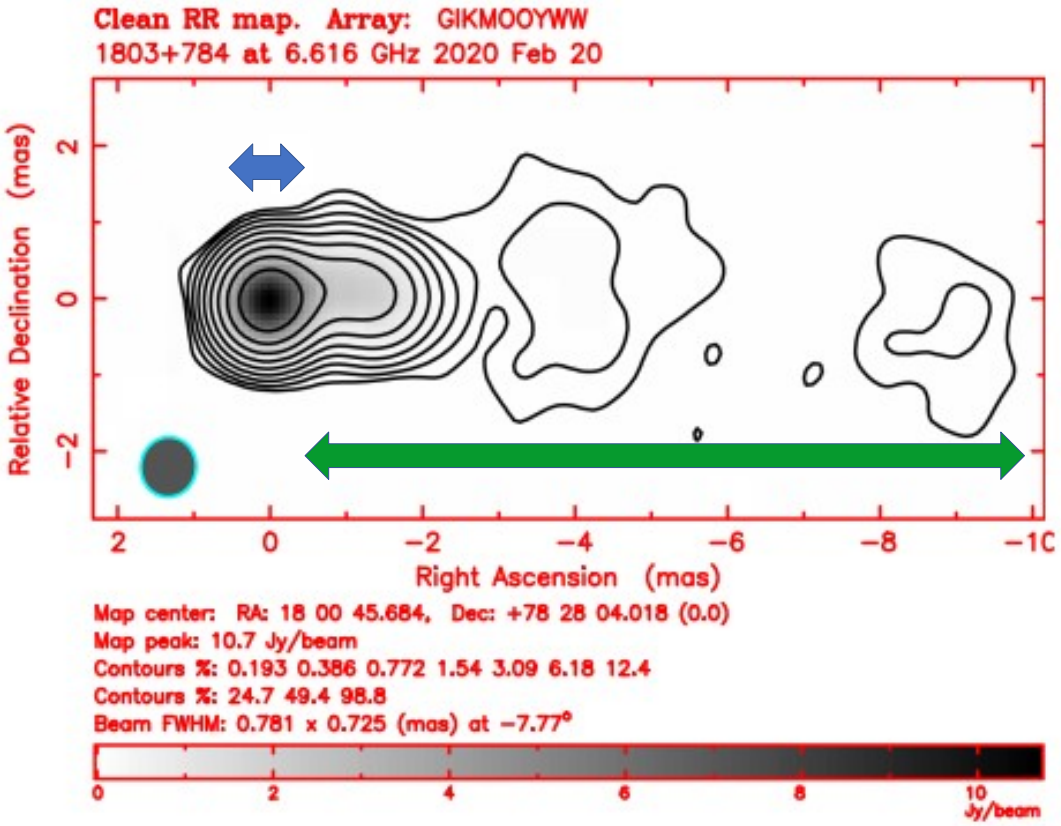

Source image of 1803+784 at 6.6 GHz from session VO0051 (Xu et al., 2021)

Structure causes two major effects:

1) **Phase center shift**
   - **Structure within the beam – "invisible" (Porcas 2010)**
   - **Source position**
2) **Systematic delay errors**
   - **Extended jet -- "visible"**
   - **Closure delays**
   - **Other geodetic parameters**

2229+695: images

2019 AUG 05

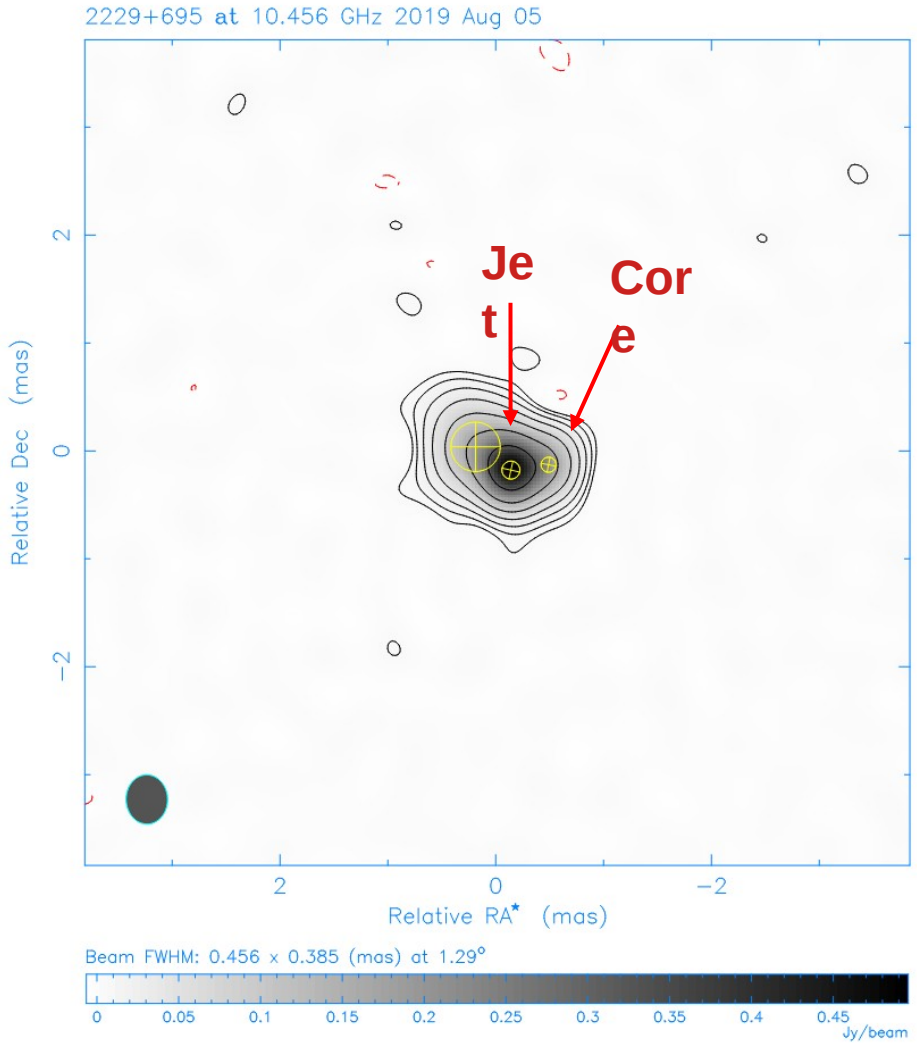

2022 JAN 27

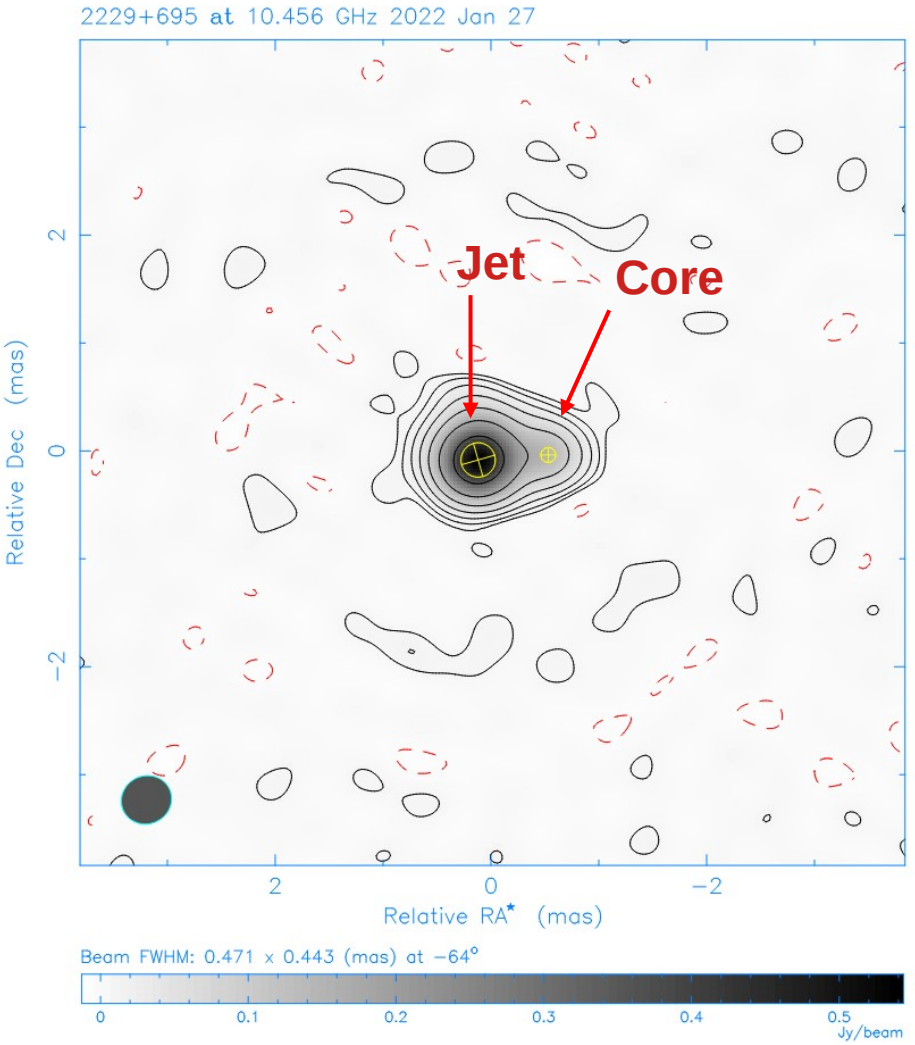

Stability of VGOS source positions

- **Source: 0059+581**

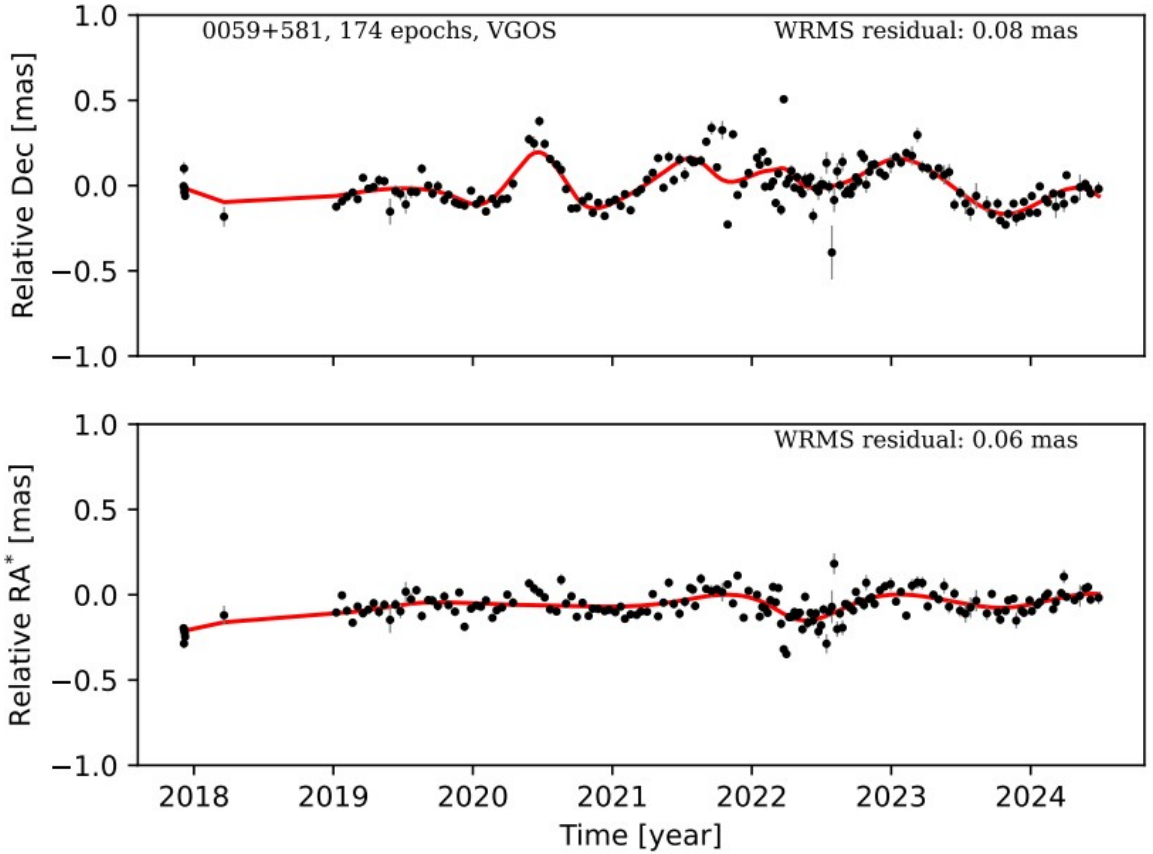

Tropospheric turbulence

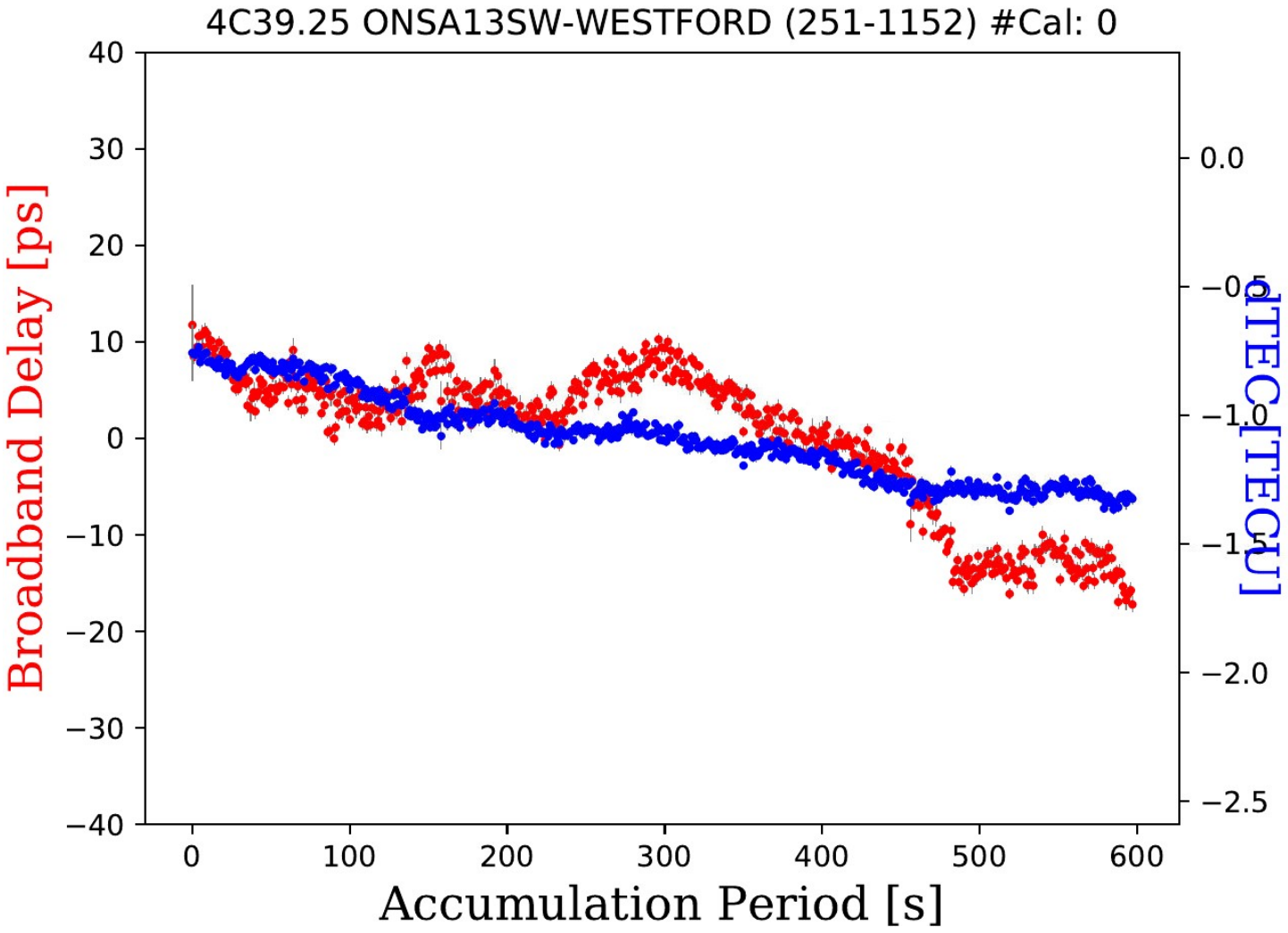

Thank you very much!

minghui.xu@gfz-potsdam.de

We are hiring!
https://www.gfz-potsdam.de/en/career/job-offers/details/9403

Data

- 177 24-hour experiments
- Simultaneously observing at four bands
- 13 VGOS antennas/fast slewing
- Short scan lengths
  - 7 – 30 seconds
- 370 radio sources

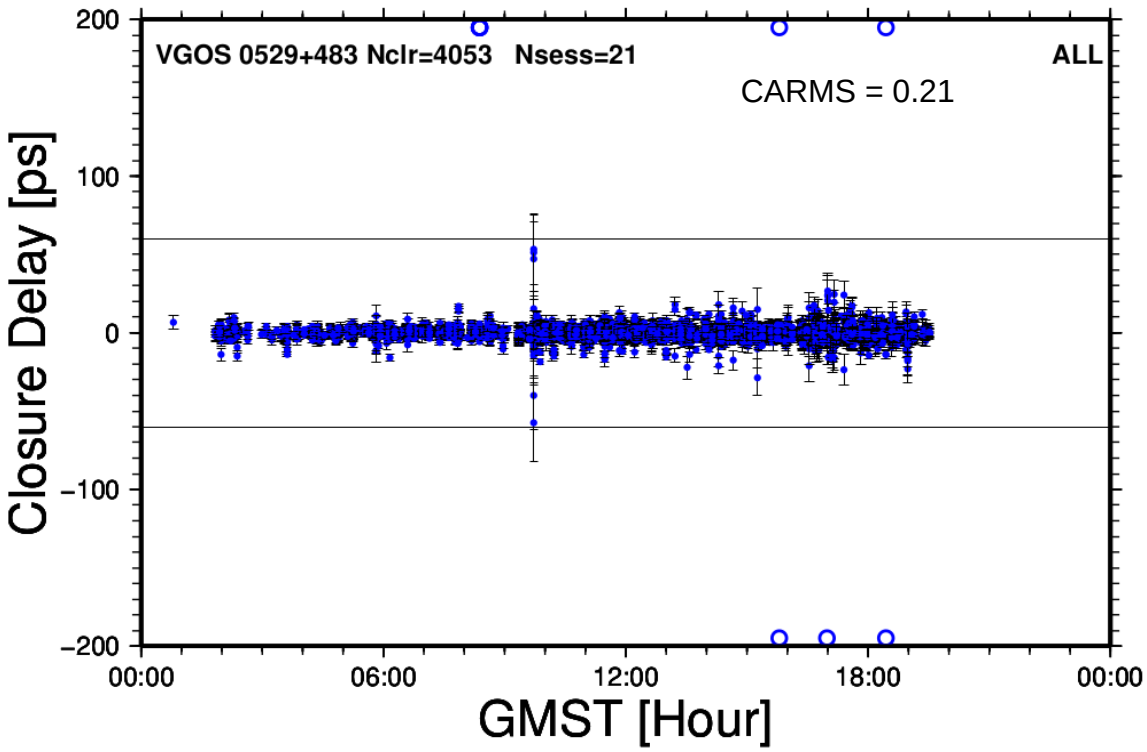

All of the closure delays of source 0529+483 in 21 VGOS sessions. WRMS = 3.0 ps

(Niell et al, 2018; Xu et al., 2021)

Stability of VGOS source positions

Impact of “invisible” structure

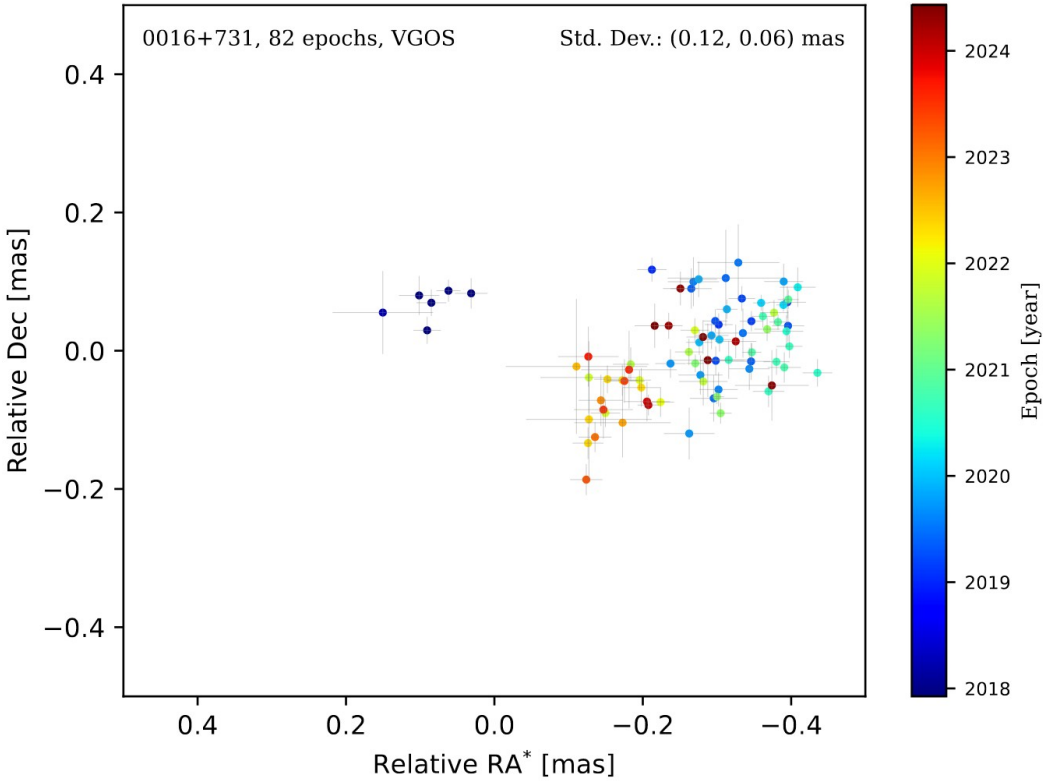

Source position variation @ 0.6 mas

Impact of “visible” structure

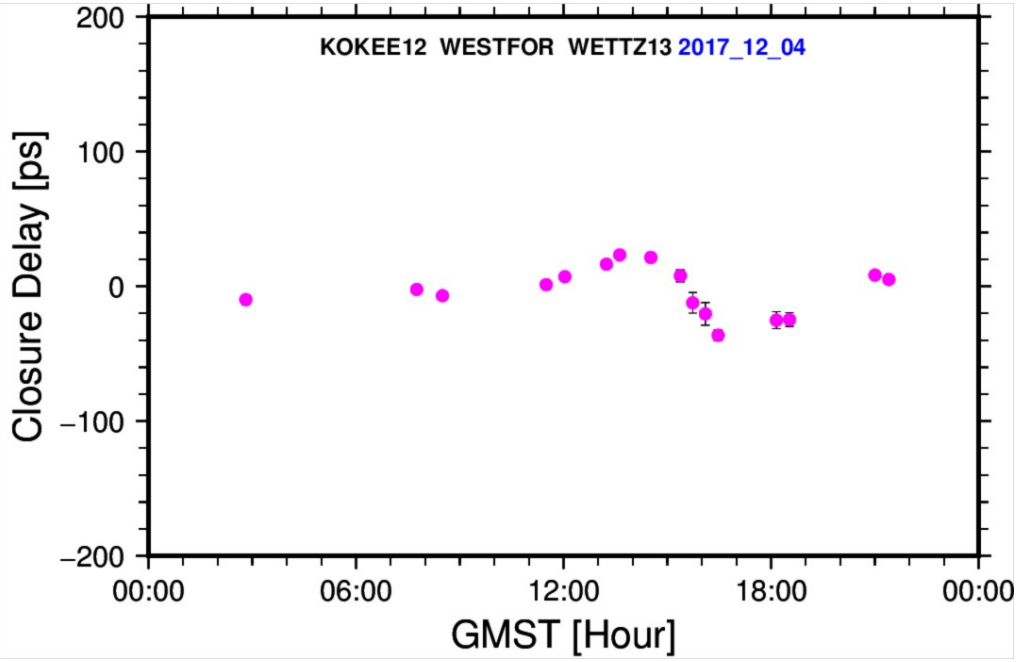

Closure delays @ 100 ps

Stability of VGOS source positions

Units: mas

	$-45°$	$-30°$	$-15°$	$0°$	$15°$	$30°$	$45°$	$60°$	$75°$	$90°$
RA*	0.32	0.20	0.13	0.08	0.05	0.05	0.05	0.05	0.04	0.03
Dec	0.47	0.36	0.26	0.19	0.13	0.09	0.06	0.05	0.04	0.04

- Error floor of VGOS source positions
- Uncertainty inflation

Sensitivity of VGOS observations to source positions

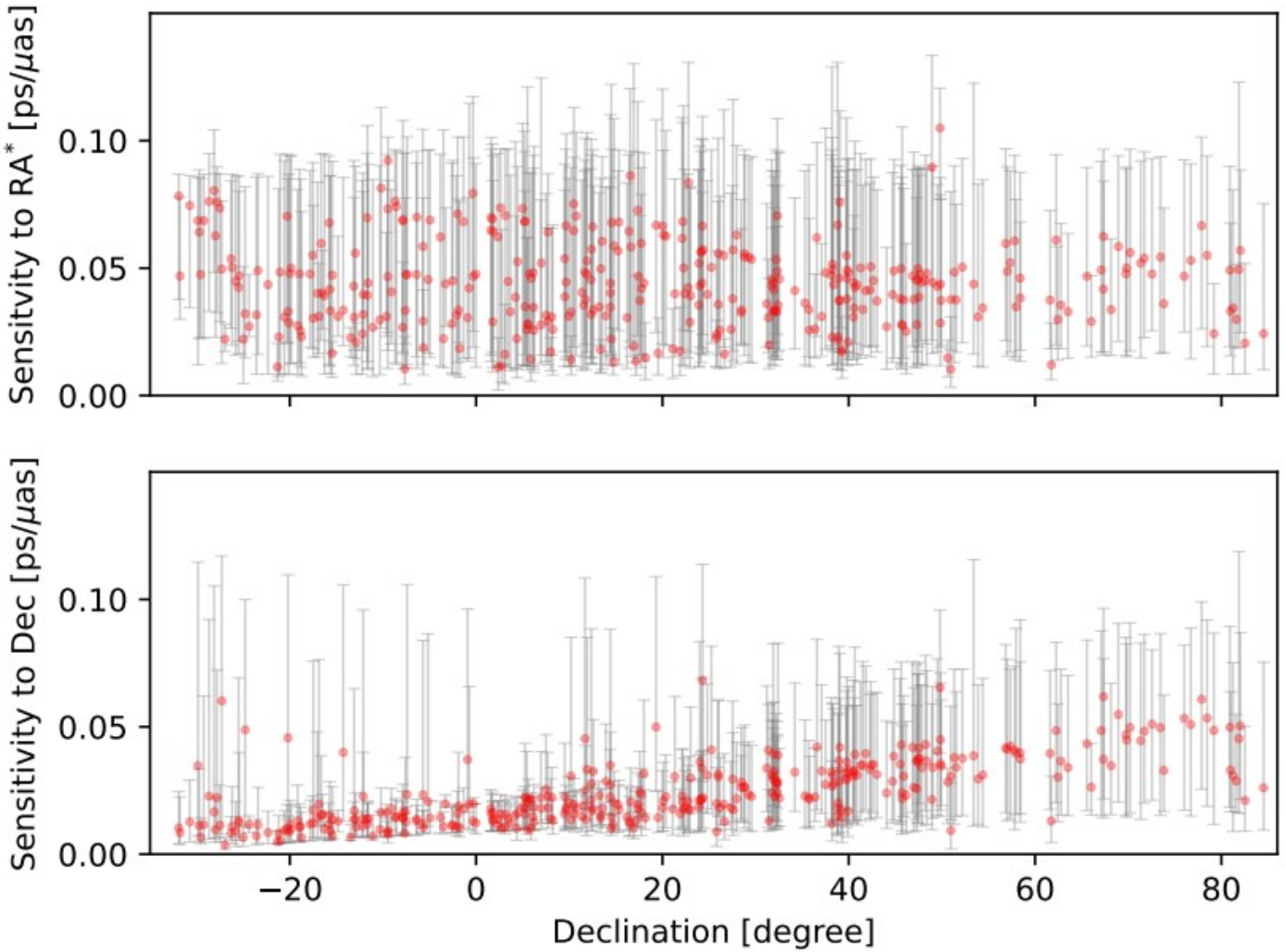

Differences between VGOS and S/X

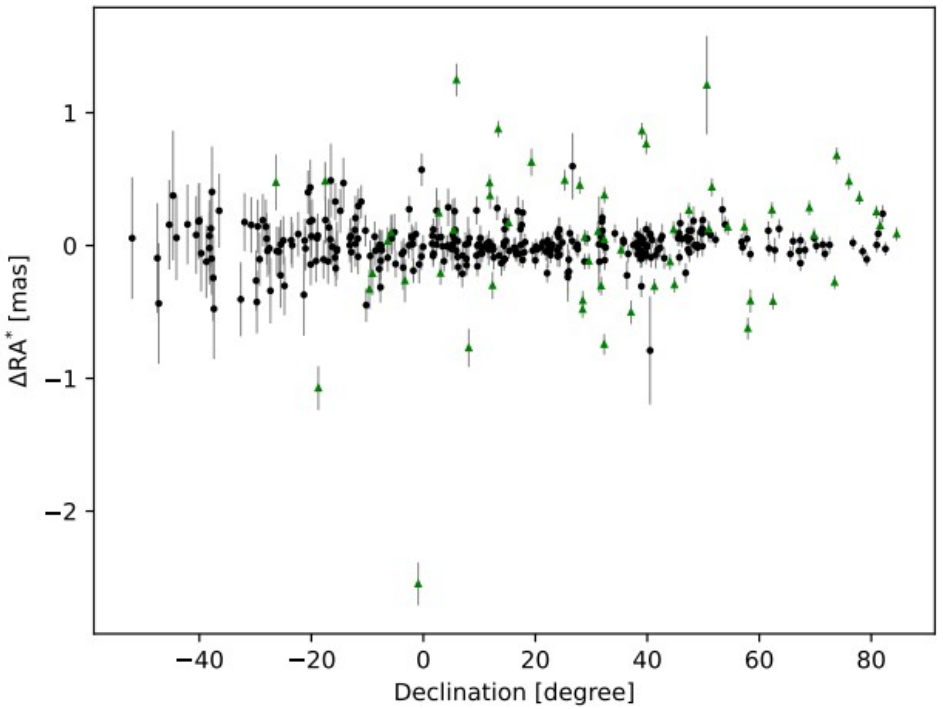

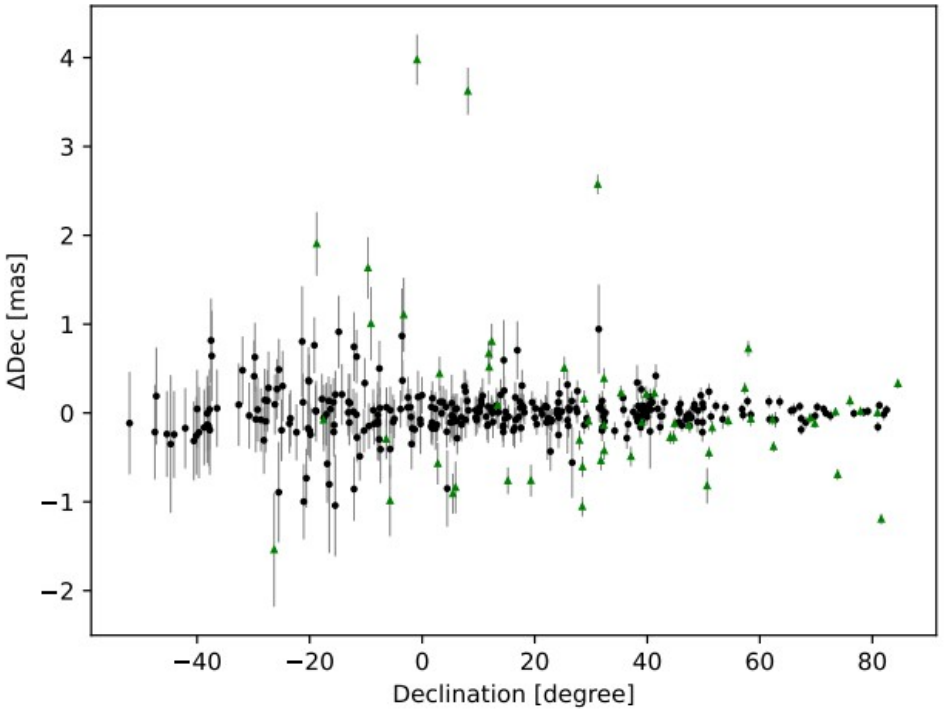

- The median and mean arc lengths over the 377 sources are 0.175 mas and 0.310 mas, respectively.

Stability of VGOS source positions

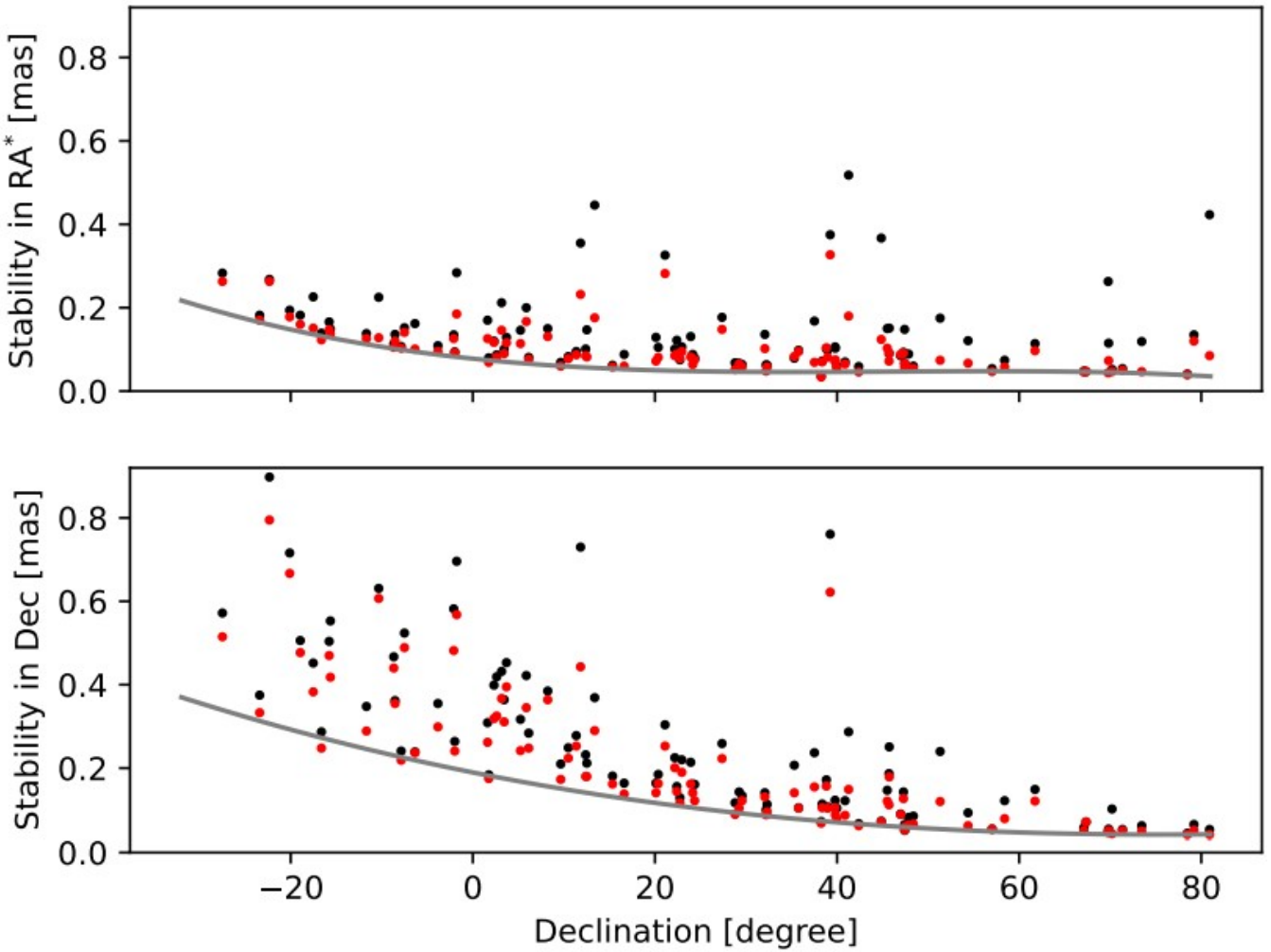

- Time variations of VGOS source position on average is:
  - 0.1 mas for sources with declination > 20 degrees
  - 0.2 mas in RA and 0.5 mas in Dec for source with declination < 20 degrees

Differences between VGOS and S/X

Source	RA [deg.]	Dec [deg.]	ΔRA^* [mas]	ΔDec [mas]	σ_{RA^*} [mas]	σ_{Dec} [mas]	Arc length [mas]	Normalized arc length
(1)	(2)	(3)	(4)	(5)	(6)	(7)	(8)	(9)
0003−066	1.5578870	-6.3931488	0.03	−0.29	0.11	0.22	0.30	3.5
0014+813	4.2853124	81.5855931	0.15	−1.19	0.06	0.06	1.20	14.3
0016+731	4.9407763	73.4583382	−0.28	0.01	0.05	0.05	0.28	6.3
0119+115	20.4233128	11.8306705	0.47	0.67	0.06	0.15	0.82	13.2
0146+056	27.3432124	5.9315466	1.25	−0.84	0.12	0.29	1.50	5.5
0202+149	31.2100579	15.2364008	0.17	−0.76	0.06	0.15	0.78	6.2
0212+735	34.3783896	73.8257281	0.68	−0.69	0.06	0.06	0.97	10.8
0229+131	37.9412255	13.3818657	0.88	0.09	0.06	0.14	0.88	10.0
0319+121	50.4712645	12.3538763	−0.30	0.80	0.10	0.20	0.86	4.5
NRAO140	54.1254481	32.3081507	−0.74	0.39	0.08	0.12	0.84	5.7
NRAO150	59.8739470	50.9639337	0.12	−0.45	0.06	0.07	0.47	7.0
0434−188	69.2561778	-18.7468366	−1.07	1.90	0.17	0.36	2.19	7.2
0454+844	77.1765149	84.5345957	0.09	0.33	0.05	0.06	0.34	4.6
0642+449	101.6334415	44.8546083	−0.30	−0.12	0.06	0.07	0.32	6.8
0650+371	103.4928450	37.0946129	−0.50	−0.49	0.09	0.11	0.70	4.7
0723−008	111.4609989	-0.9157053	−2.55	3.98	0.16	0.28	4.72	16.5
0738+313	115.2945971	31.2000644	0.11	2.57	0.08	0.11	2.58	21.2

- 15% sources have significant position offsets.